RESEARCH PAPER

Nano-Silica Coatings and their Effect on the Hydrophobicity and Electrical Properties of Power Line Porcelain Insulators

Saeid Baghshahi*, Mahnaz Dashti, Arman Sedghi, Hoda Nourmohammadi Miankoshki

* baghshahi@eng.ikiu.ac.ir

Department of Materials Engineering, Faculty of Engineering, Imam Khomeini International University, Qazvin, Iran

Abstract: The power line insulators are permanently exposed to various environmental pollutants such as dust and fine particles. This may lead to flashovers and therefore widespread power blackouts and heavy economic damage. One way to overcome this problem is to make the insulator surface superhydrophobic. In this research, the superhydrophobic properties of the insulators were improved by applying room-temperature cured composite coatings consisting of epoxy and hydrophobic nano-silica particles. Either octadecyl trichlorosilane (ODTS) or hexamethyldisilazane (HMDS) was used to coat the silica nanoparticles and make them hydrophobic. Then, the hydrophobic silica was added to a mixture of epoxy resin and hardener. The suspension was applied on the surfaces of a commercial porcelain insulator and cold-cured at ambient temperature. The coating increased the water contact angle from 50° to 149°. The samples preserved their hydrophobic properties even after 244 h exposure to the UV light. The coating adhesion was rated as 4B according to the ASTM D3359 standard. The coating decreased the leakage current by 40% and increased the breakdown voltage by 86% compared to the uncoated sample, and it showed promise for making power line insulators self-clean.

Keywords: Ceramic Insulator, Flashover, Hydrophobic Coating, Nano silica.

1. INTRODUCTION

In polluted and humid areas, the deposited pollution on insulator surfaces causes the formation of thin electrolytic conductive layers on the surfaces [1]. This conductive path forms due to the high potential difference around the current cables connected to the insulator. This current leakage and the formation of dry band arcs lead to insulator failure and power cuts. The discharge of current occurs in two forms; electric arcs or creep currents, which ultimately destroy the insulator and interrupt the electric current [2]. Common methods of washing and removing pollution and moisture are expensive and short-lived. Therefore, it is necessary to use a method that can provide water repellency or so-called hydrophobicity, and thus cleanliness on insulator surfaces.

1.1. The Science Behind Hydrophobicity and the Lotus Effect

The term hydrophobic comes from two Greek words: hydro (water) and phobos (fear). Hydrophobicity refers to the physical property of a material that repels water [3]. Hydrophobic materials are characterized by having low surface energy, meaning they do not readily interact with water molecules [4]. This can be attributed to the molecular structure of these materials, which typically consist of nonpolar or weakly polar components.

When a droplet of water lands on a hydrophobic surface, it forms a nearly spherical shape due to the cohesive forces between its molecules [5]. These forces cause the droplet's surface tension to overcome any adhesive forces between it and the surface underneath it. As a result, instead of spreading out over the surface as it would on a hydrophilic material (one that attracts water), it beads up into droplets that roll off easily.

This phenomenon is commonly encountered in nature, where plants and animals have evolved mechanisms to prevent moisture from sticking to their surfaces. One such example is the lotus plant, which has inspired scientists and engineers for decades due to its remarkable ability to remain dry and clean even when submerged in mud and dirty water.

The lotus effect is named after the lotus plant's unique ability to repel dirt and moisture from its leaves. When rain falls on a lotus leaf, rather than being absorbed or sticking around as puddles, it quickly rolls off, taking any dirt particles with it along with anything else on top. Scientists have discovered that this self-cleaning mechanism is in part due to the hierarchical micro/nanoscale intrusions called papillae covering each leaf

1

epidermis combined with wax-like compounds secreted onto them creating an uneven surface making adhesion difficult for most substances including liquids.

As previously mentioned, this natural phenomenon has inspired researchers worldwide who aim at developing new technologies that mimic the lotus effect. Applications of this technology include self-cleaning coatings, anti-icing surfaces, and even waterproof fabrics.

Hydrophobicity and the lotus effect are fascinating scientific phenomena with numerous applications in various fields. From preventing moisture damage to creating innovative products, these properties have inspired researchers for decades and will continue to do so in the future as they seek new ways to harness their potential.

1.2. Methods for Creating Super Hydrophobic Surfaces

The development of superhydrophobic surfaces has been achieved through two primary approaches, i.e., top-down and bottom-up methods [6].

1.2.1. Top-Down approach

The top-down approach involves modifying an existing surface structure by etching or coating it with hydrophobic materials [6]. This method is widely used because of its simplicity, cost-effectiveness, and ease of implementation. Surface modification techniques like laser ablation, micro-machining, photolithography, sandblasting, templating, and leaching can be used to create hierarchical structures on a material's surface that promote superhydrophobicity.

Laser ablation is one technique used in the top-down approach to create micro/nanostructured surfaces that exhibit superhydrophobic properties [7]. Researchers have used femtosecond laser pulses to generate periodic arrays on metal substrates such as copper [8]. The resulting structures had a hierarchical pattern consisting of nanospikes (30-50 nm) on microspikes (10 μm). The contact angle was measured at around 165°.

Micro-machining techniques like photolithography are also commonly employed in creating micro/nanostructures on surfaces. Liu et al. created silicon-based substrates using PECVD followed by deep reactive ion etching (DRIE) [9]. Such structures mimic natural lotus leaves' roughness range from 100 nm to several micrometres in diameter/depth resulting in high contact angle values (~160°), low sliding angles (< 5°), and excellent self-cleaning abilities.

By creating nanograsses on the surface of silicon, Shieh and his colleagues [10] created surfaces with superhydrophobic properties, with a large contact angle and low friction. First, the nanocolumns were created using the electron beam lithography process and dry etching, then they were converted into nano grass using the hydrogen plasma etching method, and finally, the hydrophobic property was created using CHF_3 plasma.

Using a combination of electron beam lithography and plasma etching, Martines and his colleagues [11] created an arrangement of low and high nanoscale structures on the surface of the material, and when this surface was covered with octadecyl trichlorosilane, the surface showed superhydrophobic properties.

Sandblasting is another technique that has been utilized for creating superhydrophobic surfaces through controlled modification of substrate morphology [12]. In this process, sand particles are blasted onto a surface under high pressure which results in the formation of random nano/microscale protrusions that increase surface roughness leading to enhanced water-repellency properties.

Qian and Shen [13] obtained superhydrophobic surfaces from polycrystalline metals (aluminum, zinc, and copper) by chemical etching. By being treated with fluorine alkyl silane, they reached a contact angle of 153°. Coulson and his colleagues [14] used the plasma etch method to roughen polytetrafluoroethyl (PTFE) substrates. He coated the substrate with polymer layers, which have low surface energy, by plasma, which increased the surface repulsion and superhydrophobic properties on the surface. Mauer and his colleagues [15] made silicon nanograsses using the process of etching and layering fluorocarbon by SF6, which reached an angle of 170°. Ming and his colleagues [16] made a superhydrophobic epoxy film with this method. First, they made a Mingamine epoxy film that had unreacted amine groups, then they coated silica particles that had amine groups on the surface of the layer and reached a suitable wetting angle. First, the silica particles were functionalized using amine groups, then they were layered on the epoxy film.

1.2.2. Bottom-up approach

The bottom-up approach involves the synthesis of new materials with tailored properties from

scratch [17, 18]. In this method, researchers use organic or inorganic compounds to form nanostructures on a substrate that exhibits superhydrophobic behavior when assembled into ordered arrays. The bottom-up methods include self-assembling monolayers (SAMs), colloidal crystal templates, chemical vapor deposition (CVD), and layer-by-layer.

SAMs can be formed by chemisorption of alkanethiols onto gold substrates which results in well-ordered layers with tunable thickness and surface chemistry. These SAMs can then be functionalized with hydrophobic groups such as perfluorinated chains to create superhydrophobic surfaces [17].

Colloidal crystal templates have also been utilized for creating periodic Nano arrays via dip-coating methods [18]. The resulting structures were highly uniform over large areas up to centimetres squared, exhibiting robust water repellency even under harsh environmental conditions.

Sun et al. [19] used a lotus leaf as a template and created a pattern by applying a layer of polydimethylsiloxane on the lotus leaf, creating a negative template. They used the negative template and applied polymethylsiloxane on it, to make a positive template. In this way, they created a super hydrophobic layer with a water contact angle (WCA) of 160°.

Zhiqing Yuan and his colleagues made the copper surface hydrophobic using a lotus leaf as a template. They reached a WCA of 153° with the same pattern, Xue and his colleagues [20] made high-density nanostructured polyethylene using an anodic aluminum oxide pattern and by adjusting its diameter and surface pressure, they made super hydrophobic polyethylene nanofibers with an angle of 160.

Ci and his colleagues [21] created rows of carbon nanotubes with a large diameter vertically on the surface and a contact angle of 170° using a chemical vapor deposition process.

Lao and his colleagues [22] modified the surface of carbon nanotubes with vertical arrangement by plasma chemical vapor deposition (PECVD) method and created a superhydrophobic surface of carbon nanotubes.

Cai and his colleagues [23] prepared hydrophobic and anti-reflective Nano silica coatings with a low reflection coefficient using the sol-gel method. They used TEOS as a starting material and MTES as an improvement of hydrophobicity. Methyl groups were substituted with hydroxyl groups and it gave hydrophobic properties. Its wetting angle was 7.108° and its radiation intensity was 1.15.

Using TEOS and MTES as coating precursors, Xu and his colleagues [24] obtained a coating with a wetting angle of 152 and a transparency of 99.8%. This angle was created due to the replacement of the hydrophobic methyl group (-CH$_3$) instead of the functional hydroxyl group (-OH) on the surface of nano-silica particles.

Philipacicius and his colleagues [25] used MTMS and HMDS as surface modifiers to create a hydrophobic nano silica coating. Better hydrophobic properties were created by using HMDS.

Ramalla and his colleagues [26] investigated the hydrophobic properties of insulators using hydrophobic nano-silica produced by the sol-gel method. A suspension of silica gel and nano-silica powder of 20-30 nanometers was applied by spraying on 3 sub-layers of bushing insulator porcelain insulator and silicon wafer. The sub-layers were annealed at 117° for 1 hour. The wetting angle was 8.158 and the hysteresis was 8°.

Su and his colleagues [27] applied the hydrophobic coating in two steps. A mixed suspension of Nano silica sol and Nano silica particles with a particle size of 20 nm was applied on the surface of the insulator. Chemical modification of the coating was done with perfluorodecyltriethoxysilane PDTS and finally, the annealing process was performed at 117°. The prepared coating had a wetting angle of 163.6° and a hysteresis of 1.4°, and the resistance to freezing was improved.

Erika et al. [28] made silica nanoparticles by sol-gel process. TEOS was combined with NH$_4$OH and hydrolyzed. HMDS was added into the tube and the resulting tube was aged. Hydrophobic nano colloidal silica was created and finally reached a wetting angle of 150.7°.

Goswami et al. [29] dissolved TEOS in methanol and added NH$_4$OH. HCl was added to it to make pH= 8 and the tube was produced and aging was done and nano-silica was created. HMDS was modified by n-Hexane and added to the composition. They applied hydrophobic Nano-silica on the surface of the glass insulator and reached a wetting angle of 168°.

Since the insulator surface has the most contact with pollution, applying a hydrophobic coating of

nano-silica particles on the surface may result in improving the [30]. Ceramic nanostructure coatings are widely used to improve surface properties and create hydrophobicity and self-cleaning, which are unique features of ceramic coatings [31].

Since many working insulators have no coating, a method must be used to apply a hydrophobic coating in situ without removing these insulators from the transmission lines and without the need for heat treatment.

One of the most effective ways to improve the performance of insulators is the use of hydrophobic coatings of silica nanoparticles. Coatings containing Nano silica particles are suitable candidates for covering the surface of insulators due to their super hydrophobic properties and resistance to aging to prevent their premature destruction and interruption of electricity flow.

One of the other methods that can be investigated and used to achieve this goal is the synthesis of cold-cured polymer composites containing hydrophobic Nano silica particles so that in addition to providing hydrophobic properties, it can also be applied in situ on the insulators of power transmission lines.

Among the various polymer materials, epoxy resin is a suitable candidate for making Nano silica composite, due to its low price, availability, high mechanical resistance, electrical current insulation, non-absorption of any dust or pollution, long-term durability on the surface, resistance to UV rays, inability to be affected by any kind of moisture, water, oil, etc. Therefore, based on the above-mentioned cases, in this research, we will apply room-temperature cured Nano-silica-epoxy hydrophobic coatings on commercial insulators to make them hydrophobic and self-clean.

2. EXPERIMENTAL PROCEDURES

2.1. Raw Materials

The raw materials used in this research and their specifications are given in Table 1.

2.2. Coating Procedure

Coating the substrates was conducted in four steps: hydrophobization of the nano-silica powder, making the nano-silica/epoxy suspension, applying the coating on a commercial 3 kV porcelain power line insulator, and cold curing the coating. The details of the coating procedure are given below.

Octadecyltrichlorosilane (ODTS) and hexamethyldisilazane (HMDS) were used to hydrophobize the silica nanoparticles. The silica nanopowders had a particle size of 20-30 nm.

To do this, 0.5 ml ODTS or HDMS was dissolved in 50 ml toluene in a round-bottom flask using a magnetic stirrer. 2 g dried nano silica powder was added to the solution and refluxed at 100°C for 24 h. Then the functionalized nano silica was filtered and dried at 110°C for 24 h.

The hydrophobic nanoparticles were added to acetone with a weight ratio of 1 to 8 mixed by a magnetic stirrer for 1 h and ultrasonicated for 30 min. Then 5 to 60 wt% hydrophobic nano silica was added to epoxy resin as an adhesive and stirred with a magnetic stirrer and ultrasound. After mixing, a hardener was added. The main reason for choosing epoxy was its special properties, such as thermal insulation, electrical insulation, good mechanical properties, high-temperature resistance, resistance to acids, and proper adhesion. Compared to self-hardening adhesives such as polyurethane, epoxy resin adhesive is more resistant to UV ray. The presence of silica nano powder also increases the UV resistance by absorbing some of the UV radiation. Before applying the coating, the surface of the insulators was washed several times with distilled water and acetone to remove any kind of dirt and grease.

Table 1. The raw materials used in this research

No.	Name	Composition	Code	Supplier	Purity (%)
1	Nano Silica	SiO_2	7631-86-9	China	99.5
2	Epoxy Resin E06	$C_{15}H_{16}O_2$	24969-06-0	China	99
3	Acetone	C_3H_6O	67-64-1	Aldrich	99.9
4	Ethanol	C_2H_5OH	64-17-5	Aldrich	80
5	Hexamethyldisilazane	$C_6H_{19}NSi_2$	999-97-3	Aldrich	99
6	Octadecyltrichlorosilane	$C_{18}H_{37}Cl_3Si$	112-04-9	Aldrich	90
7	toloene	$C_6H_5CH_3$	108-88-3	Aldrich	99

Then the hydrophobic coating was immediately applied on the insulator surface using a spraying gun. To cure and stabilize the coating, it was kept at room temperature for 24 h.

2.3. Characterization and Property Measurement

Fig. 1 shows the methods of characterizing and property measurement used in this research.

The hydrophobicity of the applied coatings was evaluated through water contact angle (WCA) measurement. This was measured using an automatic video contact-angle testing apparatus (Krüss model DSA 100 Expert). Besides the WCA measurement, the hydrophobicity class of the coatings was also determined according to the IEC TS62073 standard. In this method, water is sprayed on the sample for 10 to 30 seconds at an angle of 45°, while maintaining a distance of 10 ± 2.5 cm from the surface of the sample, and then its hydrophobicity class (HC) is determined according to Table 2 [32].

X-ray diffraction (XRD, Philips, Model 1730PW with an accelerating voltage of 40 kV and a current of 30 mA), Fourier transform infrared spectroscopy (FTIR, Thermo Co., Model Avatar), Field emission scanning electron microscopy (FESEM, Tescan, Model Mira3), and Atomic force microscopy (AFM, Csinstruments Co., Model Observer-Nano) were used to study the phase composition, the chemical bonds and functional groups, and the microstructure, and topography of the coated samples, respectively.

Fig. 1. Characterization methods to characterize the coated samples

Table 2. The criteria for evaluation of HC [32].

HC	Description
1	Only discrete droplets are formed. $\theta = 80°$ or larger for the majority of droplets.
2	Only discrete droplets are formed. $50° < \theta < 80°$ for the majority of droplets.
3	Only discrete droplets are formed. $20° < \theta < 50°$ for the majority of droplets. Usually, they are no longer circular.
4	Both discrete droplets and wetted traces from the water runnels are observed. (i.e. $\theta = 0°$). Completely wetted areas < 2 cm². Together they cover < 90% of the tested area.
5	Some completely wetted areas >2 cm², which cover < 90% of the tested area.
6	Wetted areas cover >90%, i.e., small un-wetted areas (spots/traces) are still observed.
7	Continuous water film over the whole tested area.

A scratch tester (FMC, Model 240) was used to measure the adhesion of the coatings to the surface, based on the ASTM D 3359 standard. To investigate the stability of the coatings against UV based on the ISO 4892-2 standard a stability test device (Lib Xi'an, Model UFT-340) with a Xenon lamp with a wavelength of 300-400 nm was employed. This test simulated the actual weather conditions on the sample. In this test, the samples were exposed to ultraviolet radiation, heat, and humidity in three rotation cycles and the changes in their properties were investigated. The samples were exposed for 72, 144, and 240 h, the latter being equivalent to 18 months in natural environmental conditions. The electrical discharge test of the 3kV porcelain power line insulators, was performed at dry and wet conditions based on DIN 42539 porcelain power line insulators discharge test. In the dry electrical discharge test, the voltage was applied between the electrodes of the insulator and gradually increased until it reached a certain value, then the insulator was kept at this voltage for one minute, and finally, the voltage increased until the electrical discharge stage. In the wet condition, a humidity of 5.9 mSiemens/cm was used. The electrical test of power frequency voltage resistance was performed according to IEC 60383 standard and the results were compared with the uncoated insulators.

The wet condition is the same as the dry condition, except that the water stream was poured on the insulator at an angle of 45°. The rainy and insulating conditions were kept at a certain voltage for 30 seconds and then the voltage was increased to the electrical discharge stage. In general, the electrical test of the insulators was conducted as an experimental electrical test, the device used was a Mess Wandler-Bau brand made in Germany. An electrical resistance test against power frequency voltage was performed according to the IEC60383 standard.

The leakage current test was performed on the coated and uncoated insulators according to the IEC 60060-1 standard. The applied humidity was 5.9 mS/cm with an angle of 45° on the insulator. The leakage current was taken by a desktop ammeter of the Leader model, manufactured in Taiwan. Leakage current research was conducted on coated and uncoated surfaces based on the IEC60060-1 standard.

3. RESULTS AND DISCUSSION

3.1. Results of Hydrophobized Silica Nanoparticles

The FTIR patterns of silica nanoparticles, and silica nanoparticles hydrophobiczed with ODTS and HDMS are compared in Fig. 2a-c. The peaks at 466.7, 801.5, and 1097.3 cm^{-1} belong to the bending vibration, symmetric stretching vibration, and asymmetric stretching vibration of the Si-O-Si bond, respectively.
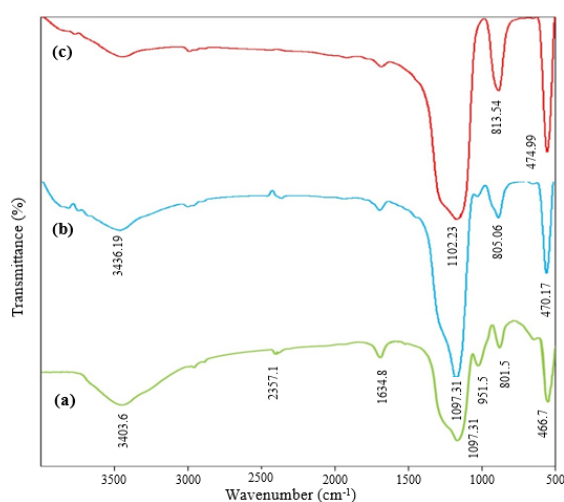
Fig. 2. The FTIR patterns of a) silica nanoparticles, b) silica nanoparticles hydrophobized with ODTS, and c) silica nanoparticles hydrophobized with HMDS

The peak at 951.5 cm^{-1} is attributed to the stretching vibration of the Si-OH bond. The peak at 1634.8 cm^{-1} is indicative of the H-O-H bending vibration bond of the water molecule. The peaks in the range of 3000-3800 cm^{-1} represent the stretching vibration of different models of hydroxyls and the remaining absorbed water [33]. The bands Si-O-Si, Si-OH, and H-O-H are indicative of unbaked silica, including Si-O bonds with surface hydroxyls (-OH).

The peak at the range of 1100-1280 cm^{-1} is related to Si-$(CH_3)_n$ bonds and the peak at 700-840 cm^{-1} is related to the bonding of Si-$(CH_3)_2$ and Si-$(CH_3)_3$, which show the presence of hydrophobic agents in silica nanoparticles [34, 35]. Fig. 3 shows the hydrophobicity of nano silica powders hydrophobized by ODTS and HDMS. It was observed that ODTS is more effective than HDMS, hence it was used to continue the research.

6

Fig. 3. The nano-silica powders hydrophobized by (A) ODTS and (B) HMDS

3.2. Results of Hydrophobized Silica Nanoparticles/Epoxy Composites

Fig. 4 shows the effect of silica loading of the coating suspension on the WCA of the coatings. As observed, the higher the silica-to-resin ratio, the higher the WCA. To have a hydrophobic surface, at least 25 wt.% silica loading is needed, and to have a superhydrophobic surface at least 35 wt% silica loading is required.

Unfortunately, with increasing the silica content, the adherence of the layer decreased. Hence, to compromise between WCA and adherence, the samples with 31, 33, and 35 wt% silica were found to be optimized. Therefore, the next stages were conducted using these three compounds, named S31, S33 and S35, respectively. They showed a WCA of 140, 150 and 151º, respectively.

The porcelain insulator, coated with 33% hydrophobic nano-silica had the hydrophobicity class of HC2 (Fig. 5) and was considered superhydrophobic based on the standard. The result obtained compared to the research of Zolriyastin et al. [36] showed a better performance.

Fig. 4. The effect of silica loading of the coating suspension on WCA

**Fig. 5.** The coated insulator after water spray

The XRD patterns of samples S31, S33, and S35 are shown in Fig. 6.

Fig. 6. The XRD pattern of the samples S31, S33 and S35.

The broad peaks seen at the 2θ angle of about 21° correspond to the amorphous plane (101) (JCPDS card 01-082-1554), indicating the presence of nano-silica particles. As the percentage of the hydrophobic silica increased, the intensity increased.

Fig. 7 shows the FESEM images of the samples S31, S33, and S35. The formed rough coating increased the effective contact surface and intensified the hydrophobicity. The presence of hierarchical micro/nano protrusions on the surface formed by the nano-silica particles, together with the non-polarity of the silica nanoparticles, almost resembles the surface of lotus leaves. The thickness of the created coating is about 52 μm. A higher thickness results in cracking and peeling due to drying shrinkage (Fig. 8).
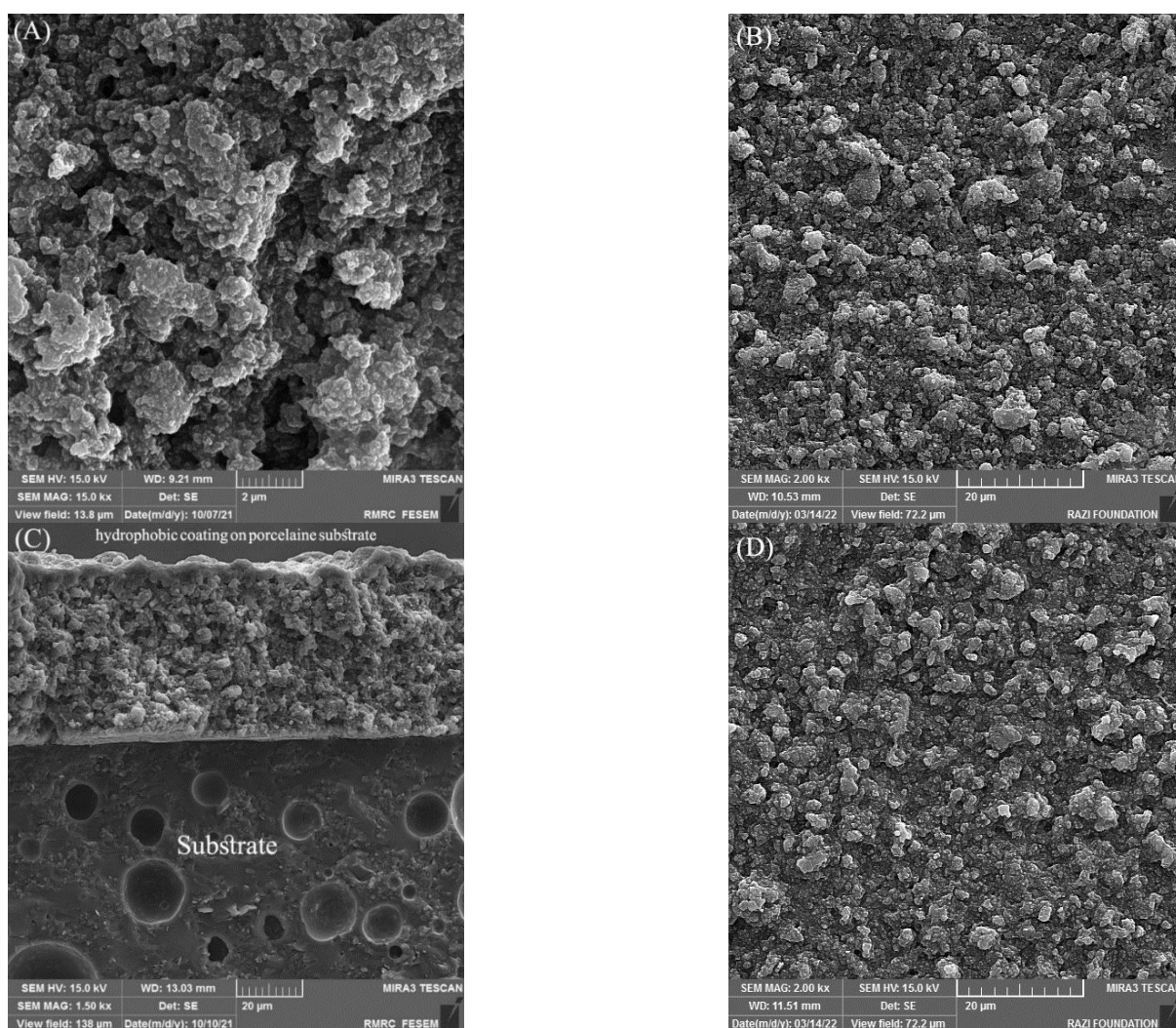

Fig. 7. FESEM images of the coatings, (A) S31, (B) S33, (D) S35, and (C) the cross-section of S33 on the glazed porcelain insulator

8

Fig. 8. Cracking and peeling of the coating, when thicker than 60 μm.

Fig. 9 and Table 3 show the topographical results of the samples, obtained by AFM. The protrusions on the surface of the samples had a height of about 1 μm. The unevenness on the surface caused by the presence of silica nanoparticles caused an increase in the specific surface area and as a result a relative increase in the hydrophobicity. In sample S33, the particles are more cohesive and the percentage of porosity of the hydrophobic silica coating has decreased and the coating has become denser. It also showed a more homogeneous distribution on the surface than the other two coatings, which is in good agreement with the field emission scanning electron microscope results.
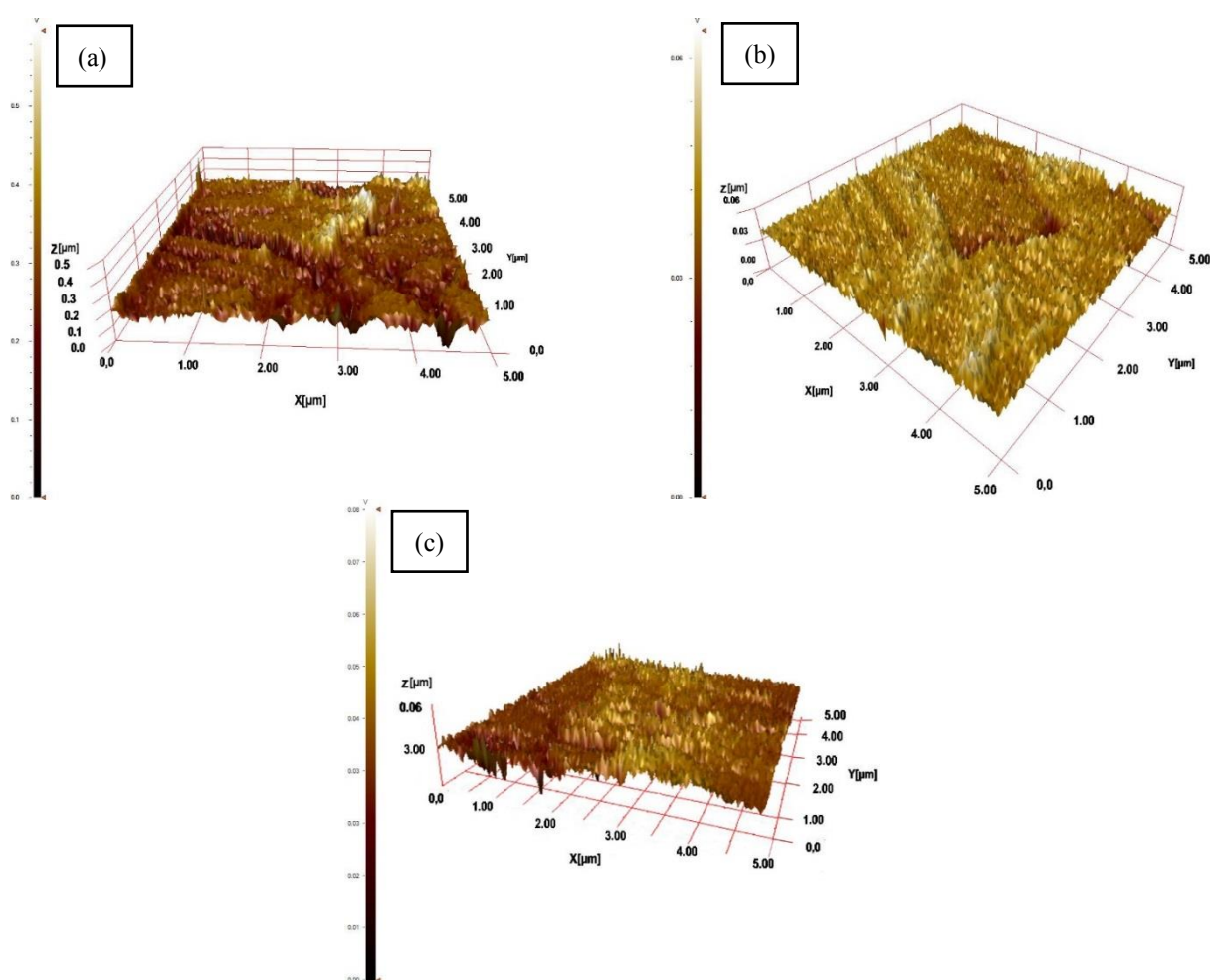
Fig. 9. AFM image of the coatings：(a) S31, (b) S33 and (c) S35

Table 3. The quantitative results of the AFM

Sample	Sa (Ra) (Roughness Average) nm	Sq (Rms) (Root Mean Square) nm	Ssk (Surface Skewness)	Sku (Rsk) (Surface Kurtosis)
S31	391.5392	506.0594	1.510673	2.466704
S33	348.7128	429.9795	1.498355	2.49667
S35	431.5392	546.0594	1.510673	2.466704

The height deviation from the average height, which is the average surface roughness (Ra), was measured. Rms is the root mean square roughness, and Rsk is the skewness parameter that shows the symmetry and flatness of the surface profile around the mean line. Now, if the height distribution is symmetrical, Rsk= 0, and if it is not symmetrical and Rsk is a positive number, the number of peaks is more than the valleys, which according to the results obtained in the coated samples, this value is positive and indicates superhydrophobicity of the surface and the successful creation of the lotus mechanism by the coating. The higher the percentage of hydrophobic silica, the bigger the Rsk, and the lower the Rms value, the smoother the sample surface. According to this fact, sample S33 has the best hydrophobicity and adhesion. Since the coating was cured at room temperature, it naturally created a relatively rough coating, but still, the average roughness of the surface was 348 nm. The Rms value of S33 is less than S35, which is indicative of the smoothness of S31 compared to S35. At the same time, it has a needle-like surface from the microscopic point of view, which is appropriate for providing superhydrophobic conditions. The presence of very thin peaks with very narrow valleys between them has caused the roughness of the surface and the creation of a hydrophobic surface on the substrate, in sample S33, peaks of the same size were created due to the uniform dispersion of silica nanoparticles on the surface. Besides, the presence of the hydrophobic CHs group on the tips of the protrusions contributed to the superhydrophobicity of the surface. In general, the more hydrophobic silica was loaded, the sharper protrusions with a shorter distance were formed, which has a direct effect on increasing the wetting angle, as a result of air pocket entrapment. The results of the adhesion test based on the ASTM D3359 standard on the surface of the coated samples S31, S33, and S35 are given in Table 4. The coatings with a higher silica nanoparticle loading have less adhesion to the substrate and vice versa. This result was expected as the resin plays the role of binder and its reduction diminishes adhesion. On the other hand, with increasing resin content, hydrophobicity is ruined, hence a compromise is necessary. It seems that in the present condition, sample S33 is the optimal sample. This type of coating does not have the adhesion problems of non-nanostructured coatings and silicone rubber that separate from the surface of the insulator after some time, and it has high strength and adhesion with the substrate [37, 38].

The effect of UV irradiation on WCA is presented in Fig. 10. As expected, before exposure, S31 and S35 had the lowest and highest WCA, respectively, corresponding to their silica content. Interestingly, long UV exposure had a minor effect on the hydrophobicity of sample S31 and a major effect on the hydrophobicity of sample S35. S31 and S33 show a slow WCA reduction after long exposure to UV. However, S35 demonstrates a sharp drop in WCA. This is believed to be due to the low adhesion of the coating, which results in peeling after long exposure. Our results show improvement compared to other researchers, e.g. Jiang et al. [39]. Their sample showed a reduction of WCA from 155 to 150°, only after 36 h exposure to UV irradiation. Also, Compared to the work of Soroori et al. [40], the hydrophobic coating of our research has been more resistant to UV rays. Their hydrophobic coating faced a decrease in hydrophobicity after 9 months. The chemistry of some coatings, such as epoxy, is very sensitive to these radiations, therefore, the resistance to ultraviolet radiation of many coatings is significantly improved with stabilizing additives, which in this research is by adding silica nanoparticles in the epoxy substrate and their presence upon the layer of epoxy chains helped to increase its resistance and stability against UV. However, the higher the amount of glue compared to nanoparticles, the lower the stability of the glue against UV. and the higher the amount of nanoparticles and the glue, the lower the adhesion is. Hence the best resistance to UV and adhesion was observed in S3.

Table 4. The adherence test of the coatings

| No.	Nano-silica content (%)	Adhesion Class
S$_1$	31	0% separation (5B)
S$_3$	33	5% separation less than (4B)
S$_5$	35	50% (0B) separation more than

Fig. 10. The Effect of UV irradiation on WCA

Ultraviolet rays only affect the epoxy paint and make the color of the epoxy resin coating yellow and amber. Still, when we use nanoparticles in its composition, it increases the mechanical strength and resistance. When the epoxy is in contact with UV for a long time, the photodegradation process occurs because the epoxy network's transverse bonds are destroyed and the physical and mechanical properties decrease. Now we have increased the resistance and strength in another way by using silica nanoparticles as a reinforcing phase next to the epoxy chain. In fact, with the passage of time and the effects of ultraviolet rays on the epoxy structure, its adhesion on the insulating porcelain substrate decreases, and when the coating is peeled off and cracked, the hydrophobicity decreases, but with the use of nanoparticles in the epoxy substrate The mechanical strength of the adhesive is increased in addition to the hydrophobicity and the hydrophobic coating is fixed on the substrate without destruction.

The best sample, S33, was tested for breakdown voltage and leakage current. The experimental setup and results are shown in Fig. 11 and Table 5, respectively. The results indicated that the hydrophobic coating on the insulator surface increased the breakdown voltage of the insulator. In the wet state, the average breakdown voltage increased from 15 kV for the uncoated sample to 28 kV for the coated sample after three repetitions. This represents a ~86% increase compared to the uncoated sample. In the dry state, the hydrophobic coating did not affect the electric discharge voltage and the corona occurrence, and the results were similar to those of the uncoated sample.
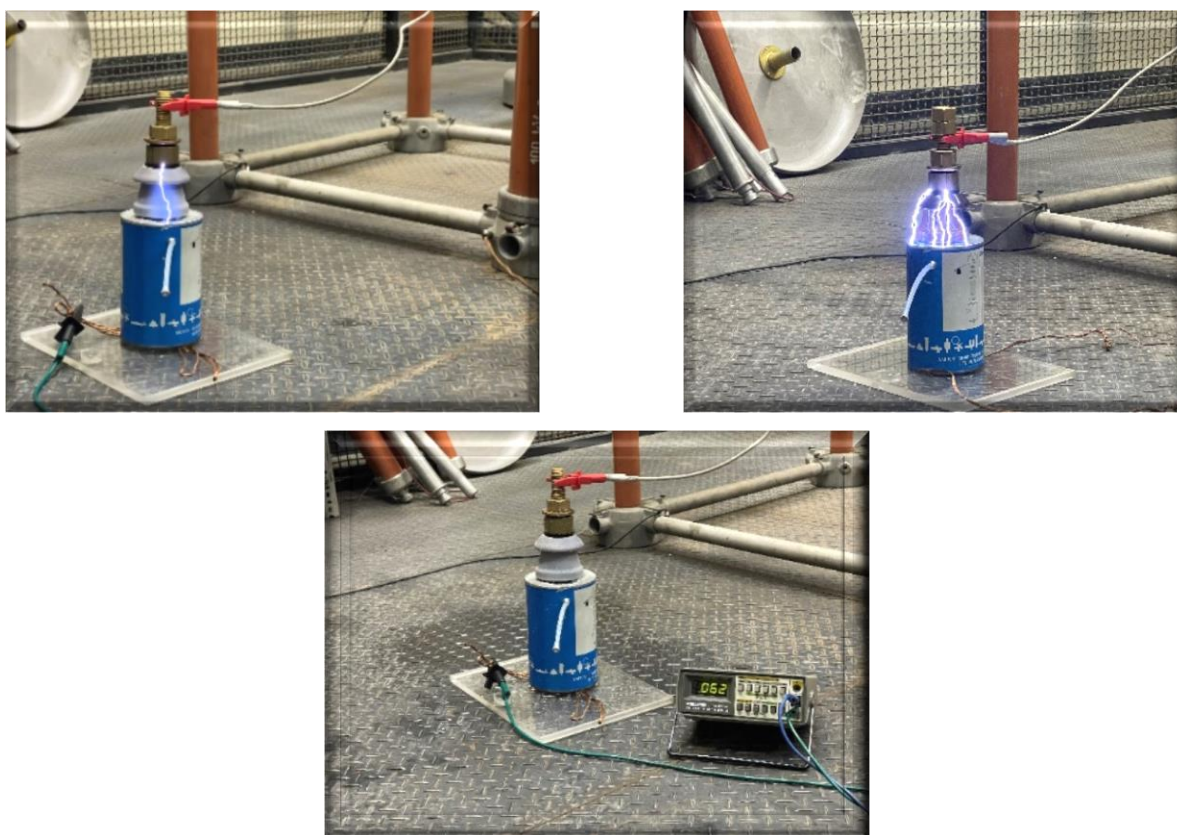
Fig. 11. The setup for the breakdown voltage test (a) the uncoated and (b) the coated (S33) samples, together with the setup for the leakage current test (c)

Table 5. The results of (a) the breakdown voltage and (b) the leakage current tests of the uncoated and coated (S33) samples

Sample	Test Conditions	Break Down Voltage (kV)	Current Leakage (µA)
Wet	Uncoated	15	103
	Coated (S33)	28	62
Dry	Uncoated	28	0.02

The breakdown voltage was 28 kV in the dry state. Under a voltage of 10 kV, the leakage current in the wet state was 103 µA for the uncoated sample and 62 µA for the coated sample (S33). This shows that the coating reduced the leakage current by 40%. Our results are better than those of many other researchers. For example, Zolriyastin et al. [36] coated insulators with nano-silica containing RTV and found no significant improvement in the leakage current (383 µA for the uncoated sample and 382 µA for the coated sample).

4. CONCLUSIONS

This research achieved the following main outcomes:

1- Hydrophobic silica-epoxy composite coatings with 5 to 60 wt% nano silica loadings were prepared, and the optimal loading was 33 wt% (S33) in terms of hydrophobicity (WCA≈ 150°) and adhesion.

2- The coating had 4B adhesion according to the standard, which means less than 5% coating separation. This solved the problem of low adhesion of RTV coating.

3- The breakdown voltage of the insulator increased from 15 to 28 kV after applying the coating.

4- The leakage current decreased from 103 to 62 µA, which was more than a 40% reduction, which improved the lifespan and performance of the insulator.

5- The UV exposure for 240 h reduced the WCA from 149 to 140, which was a ~6% reduction, indicating the excellent weathering resistance of the coatings.

6- The FESEM and AFM studies showed that the coatings had good homogeneity and integrity, with a suitable roughness for hydrophobicity, and a microscopic needle-shaped structure that explained the superhydrophobicity of the coating.

In summary, the composite coating of 33% superhydrophobic nano silica-epoxy with a particle size of 20-30 nm of silica and a surface roughness of less than 52 nm had good hydrophobic properties for porcelain insulators. The coating did not show a noticeable decrease in hydrophobicity over time due to aging or pollution accumulation. Therefore, the results of this research suggest a promising future for the improvement and progress of the energy industry.

DATA AVAILABILITY

The data that support the findings of this study are available from the corresponding author.

REFRENCES

[1] Singh, S. N., Electric Power Generation: Transmission and Distribution, Prentice Hall of India; 2nd ed., 2008.

[2] Mavrikakis, N., Siderakis, K. and Mikropoulos, P. N., "Laboratory Investigation on Hydrophobicity and Tracking Performance of Field-Aged Composite Insulators" 49th International Universities Power Engineering Conference (UPEC), Cluj-Napoca, Romania, 2014, 1-6.

[3] Daoud, W. A., Self-Cleaning Materials and Surfaces: A Nanotechnology Approach, John Wiley and Sons, NY, USA, 2013.

[4] Cassie, A. B. D. and Baxter, S., "Wettability of Porous Surfaces." Trans. Faraday Soc., 1944, 40, 546-551.

[5] Rajabi, M., "An Overview of Self-Cleaning Coatings", Scientific-specialized quarterly of the student scientific association of the faculty of polymer and paint engineering, Amir Kabir University of Technology, 2013.

[6] Liu, Y., Superhydrophobic Surfaces for

Electronic Packaging and Energy Applications, Ph.D. Thesis, Georgia Institute of Technology, 2013.

[7] Wu, B., Zhou, M., Li, J., Ye, X., Li, G. and Cai, L., "Superhydrophobic Surfaces Fabricated by Microstructuring of Stainless Steel Using a Femtosecond Laser." Appl. Surf. Sci., 2009, 256, 61-66.

[8] Levinas, R., Grigucevičienė, A., Kubilius, T., Matijošius, A., Tamašauskaitė-Tamašiūnaitė, L., Cesiulis, H. and Norkus, E., "Femtosecond Laser-Ablated Copper Surface as a Substrate for a MoS2-Based Hydrogen Evolution Reaction Electrocatalyst." Mater., 2022, 15, 3926-3933.

[9] Liu, H., Du, Y., Yin, X., Bai, M. and Liu, W., "Micron/nanostructures for Light Trapping in Monocrystalline Silicon Solar Cells." J. Nanomater., 2022, 3, 1-40.

[10] Shieh, J., Hou, F. J., Chen, Y. C., Chen, H. M., Yang, S. P., Cheng, C. C. and Chen, H. L., "Robust Airlike Superhydrophobic Surfaces." Adv. Mater., 2010, 5, 597-601.

[11] Martines, E., Seunarine, K., Morgan, H., Gadegaard, N., Wilkinson, C.D. and Riehle, M. O., "Superhydrophobicity and Superhydrophilicity of Regular Nanopatterns.", Nano Lett., 2005, 5, 2097-2103.

[12] Sun, R., Zhao, J. Li, Zh. Mo, J. Pan, Y., Luo D. B., "Preparation of Mechanically Durable Superhydrophobic Aluminum Surface by Sandblasting and Chemical Modification." Prog. Org. Coat., 2019, 133, 77-84.

[13] Qian, B. and Shen, Z., "Fabrication of Superhydrophobic Surfaces by Dislocation-Selective Chemical Etching on Aluminum, Copper, and Zinc Substrates." Langmuir, 2005, 21, 9007-9009.

[14] Coulson, S. R., Woodward, I., Badyal, J. P. S., Brewer, S. A. and Willis, C., "Super-Repellent Composite Fluoropolymer Surfaces." J. Phys. Chem. B, 2000, 104, 8836-8840.

[15] Mauer, J. L., Logan, J. S., Zielinski, L. B. and Schwartz, G. C., "Mechanism of Silicon Etching by a CF4 Plasma." J. Vac. Sci. Tech., 1978, 15, 1734-1738.

[16] Ming, W., Wu, D., van Benthem, R. A. T. M. and De With, G., "Superhydrophobic Films From Raspberry-Like Particles." Nano Lett., 2005, 5, 2298-2301.

[17] Tam-Chang, S. W., Biebuyck, H. A., Whitesides, G. M., Jeon, N. and Nuzzo, R.G., "Self-Assembled Monolayers on Gold Generated from Alkanethiols with the Structure RNHCOCH2SH." Langmuir, 1995, 11, 4371-4382.

[18] Si, Y., Dong, Z. and Jiang, L., "Bioinspired Designs of Superhydrophobic and Superhydrophilic Materials." A.C.S. Centr. Sci., 2018, 4, 1102-1112.

[19] Sun, M., Luo, C., Xu, L., Ji, H., Ouyang, Q., Yu, D. and Chen, Y., "Artificial Lotus Leaf by Nanocasting." Langmuir, 2005, 21, 8978-8981.

[20] Xue, C. H., Jia, S. T., Zhang, J. and Ma, J. Z., "Large-Area Fabrication of Superhydrophobic Surfaces for Practical Applications: An Overview." Sci. Tech. Adv. Mater., 2010, 11, 033002.

[21] Ci, L., Vajtai, R. and Ajayan, P. M., "Vertically Aligned Large-Diameter Double-Walled Carbon Nanotube Arrays Having Ultralow Density." J. Phys. Chem., C, 2007, 111, 9077-9080.

[22] Lau, K. K., Bico, J., Teo, K. B., Chhowalla, M., Amaratunga, G. A., Milne, W. I., McKinley, G. H. and Gleason, K. K., "Superhydrophobic Carbon Nanotube Forests." Nano Lett., 2003, 3, 1701-1705.

[23] Cai, S., Zhang, Y., Zhang, H., Yan, H., Lv, H. and Jiang, B., "Sol-Gel Preparation of Hydrophobic Silica Antireflective Coatings with Low Refractive Index by Base/Acid Two-Step Catalysis." ACS Appl. Mater. Interf., 2014, 6, 11470-11475.

[24] Xu, J., Liu, Y., Du, W., Lei, W., Si, X., Zhou, T., Lin, J. and Peng, L., "Superhydrophobic Silica Antireflective Coatings with High Transmittance via a One-Step Sol-Gel Process." Thin Sol. Films, 2017, 631, 193-199.

[25] Philipavičius, J., Kazadojev, I., Beganskienė, A., Melninkaitis, A., Sirutkaitis, V. and Kareiva, A., "Hydrophobic Antireflective Silica Coatings via Sol-Gel Process." Mater. Sci., 2008, 14, 283-287.

[26] Ramalla, I., Gupta, R. K. and Bansal, K., "Effect on Superhydrophobic Surfaces on Electrical Porcelain Insulator, Improved Technique at Polluted Areas for Longer

Life and Reliability." Internat. J. Eng. Tec., 2015, 4, 509-517.

[27] Su, R., Liu, H., Kong, T., Song, Q., Li, N., Jin, G. and Cheng, G., "Tuning Surface Wettability of Inx Ga(1–X)N Nanotip Arrays by Phosphonic Acid Modification and Photoillumination." Langmuir, 2011, 27, 13220-13225.

[28] Kiele, E., Senvaitiene, J., Grigucevičienė, A., Ramanauskas, R., Raudonis, R. and Kareiva, A., "Sol-Gel-Derived Coatings for the Conservation of Steel." Proc. Appl. Ceram., 2015, 9, 81-89.

[29] Goswami, D., Medda, S.K. and De, G., "Superhydrophobic Films on Glass Surfaces Derived from Trimethylsilanized Silica Gel Nanoparticles." ACS Appl. Mater. Interf., 2011, 3, 3440-3447.

[30] Marsal, A., Ansart, F., Turq, V., Bonino, J. P., Sobrino, J.M., Chen, Y.M. and Garcia, J., "Mechanical Properties and Tribological Behavior of a Silica or/and Alumina Coating Prepared by Sol-Gel Route on Stainless Steel." Sur. Coat. Tech., 2013, 237, 234-240.

[31] Riahi, N., Sarpoolaki, H., Mahdikhani, A., "Applying Ceramic Nano Coating on 120 kN Porcelain Insulators and Checking Electrical Properties" 22nd International Electricity Conference, Tehran, Iran, 2016.

[32] Jayabal, R., Vijayarekha, K. and Rakesh Kumar, S., "Design of ANFIS for Hydrophobicity Classification of Polymeric Insulators with Two-Stage Feature Reduction Technique and its Field Deployment", Energies, 2018, 11, 3391-3398.

[33] Deniz, S. and Arikan, B., "Effect of Silica Type on Superhydrophobic Properties of PDMS-Silica Nanocomposite Coatings." Inter. J. Eng. Appl. Sci., 2016, 8, 19-27.

[34] Haukka, S. and Root, A., "The Reaction of Hexamethyldisilazane and Subsequent Oxidation of Trimethylsilyl Groups on Silica Studied by Solid-State NMR and FTIR.", J. Phys. Chem., 1994, 98, 1695-1703.

[35] Jayabal, R., Vijayarekha, K. and Rakesh Kumar, S., "Design of ANFIS for Hydrophobicity Classification of Polymeric Insulators with Two-Stage Feature Reduction Technique and its Field Deployment." Energies, 2018, 11, 3391-3399.

[36] Zolriasatein, A., Rajabimashhadi, Z., Abyazi, S. and Rezaei, M., "Coating and Testing of 70 kN Ceramic Insulators with Silicon Materials Containing Silica Nanoparticles" The 7th National Conference on Nanotechnology in the Electricity Industry, Niroo Research Institute, Tehran, Iran, 2019.

[37] Hosseini Nesab, F., "Application of Nanotechnology in the Insulation Industry." Collect. Ind. Rep. Nanotech., 2014, 14, 76-85.

[38] Jazayeri, S. H., Ehsani, M., and Farhang, F., "Investigating the Role of RTV Silicone Coatings in Improving the Behavior of Ceramic Insulators in Polluted Environments." J. Color Sci. Tech., 2017, 1, 9-22.

[39] Jiang, T. and Guo, Z., "Robust Superhydrophobic Tungsten Oxide Coatings with Photochromism and UV Durability Properties." Appl. Surf. Sci., 2016, 387, 412-418.

[40] Soroori, P., Baghshahi, S., Kazemi, A., Riahi Noori, N., Payrazm, S. and Aliabadizadeh, A., "Room Temperature Cured Hydrophobic Nano-Silica Coatings for Outdoor Insulators Installed on Power Lines without Shutting Down the Current." Iran. J. Mater. Sci. Eng., 2022, 19 (3), 1-12.